Form-finding of nonregular tensegrity systems

Li Zhang, Bernard Maurin, René Motro

Form-Finding of Nonregular Tensegrity Systems

Li Zhang[1]; Bernard Maurin[2]; and René Motro[3]

Abstract: The potential applications of tensegrity structures are not only increasing in civil engineering but also in fields like biomechanics. The key step in designing tensegrity, the form-finding problem, has been investigated by many researchers but until now they have tended to focus on methods for regular shapes. Since there is an increasing need for design tools devoted to more various and complex systems, the objective of this paper is to present the form-finding of nonregular tensegrity structures with a numerical approach. It is based on the dynamic relaxation method with kinetic damping, and new tensegrity configurations in more intricate and creative forms can be obtained this way. During the form-finding process, either the force or length of some elements can be fixed by an appropriate choice of related stiffnesses. The application of the process is illustrated by several numerical examples. It can be concluded that an improvement in tensegrity form-finding has been achieved extending research from regular shapes toward "freer" shapes.

Keywords: Stiffness; Structural analysis; Shape.

Introduction and Objectives

Tensegrity systems, according to the definition given by Motro (2003), may be described as follows: "A tensegrity system is a system in a stable self-equilibrated state comprising a discontinuous set of compressed components within a continuum of tensioned components." Like many self-stressed reticulated systems, tensegrity structures are attractive since they represent lightweight systems and the transparency they convey provides new sources of inspiration for architects and civil engineers (Fest et al. 2004; Motro 2003; Sultan and Skeleton 2003).

At the same time, biologists have shown that a pertinent modeling for the mechanical behavior of the cytoskeleton of living cells can be obtained by tensegrity systems (Ingber 1997; Stamenović 2005). The cytoskeleton (see Fig. 1) is a structure composed of different polymer filaments in traction (microfilaments) and in compression (microtubules) and their prestress acts on the rigidity of the cell and finally on its metabolism. However, the geometry and topology of the filament nets are complex, even chaotic, and current tensegrity models do not fit such configurations. Researchers are therefore looking for new methods allowing the design of tensegrity structures with complex shapes. In the "Laboratory of Mechanics and Civil Engineering" (University Montpellier 2) and in the "Lightweight Structures for Architecture" research group (School of Architecture Languedoc-Roussillon), various nonregular physical tensegrity models have been built (some are shown in Fig. 2). The first was called "cloud" by Motro, clearly suggesting that such a system relies on "free form" tensegrity.

At this point it is useful to classify tensegrity systems into three types: First, regular systems characterized by all the cable elements being of the same length, let us say "*c*", and all the strut elements of the same length "*s*" (the "Simplex" is the best known); second, semiregular systems that present a minimal number of different lengths, that is to say the fewest possible groups, a group being composed of identical length elements; and finally, nonregular systems where no constraint on the lengths is specified.

The major obstacle in the design of a tensegrity structure is related to determining its equilibrium configuration, which is known as form-finding. Two main form-finding groups classified as "form controlled" or "force controlled" have been proposed. The first is illustrated by the work carried out by several people, in particular the sculptor K. Snelson (Motro et al. 2002). The equilibrium and stability of the systems he created were based on a heuristic approach with experimentation on a trial and error basis. This occasionally gave very impressive results; we used this approach to generate the models presented in Fig. 2. The second group was developed using theoretically modeled form-finding methods to meet the mechanical requirements. Several procedures have been proposed, initially based on static equilibrium methods but currently dealing with the force density method and dynamic relaxation technique (Motro 2003; Williamson et al. 2003; Nishimura and Murakami 2001; Sultan et al. 2001).

The force density method has shown its efficiency in determining regular shapes, even if the choice of the force density coefficients often proves to be difficult. A unique set of coefficients is associated with every equilibrated system with the result that an arbitrary or nonadapted choice is more likely to fail than to converge to a solution. A multiparametered approach has been proposed to try to overcome this issue and to investigate irregular shapes (Vassart and Montro 1999). This is mathematically based on the control of the rank of the "connectivity coefficient matrix." However, it works for simple systems like triplex or quadruplex

[1]Post Doctoral Candidate, Laboratoire de Mécanique et Génie Civil, Univ. Montpellier 2, CC 48, Pl. Bataillon, 34095 Montpellier Cedex 5, France.

[2]Assistant Professor, Laboratoire de Mécanique et Génie Civil, Univ. Montpellier 2, CC 48, Pl. Bataillon, 34095 Montpellier Cedex 5, France (corresponding author). E-mail: maurin@lmgc.univ-montp2.fr

[3]Professor, Laboratoire de Mécanique et Génie Civil, Univ. Montpellier 2, CC 48, Pl. Bataillon, 34095 Montpellier Cedex 5, France.

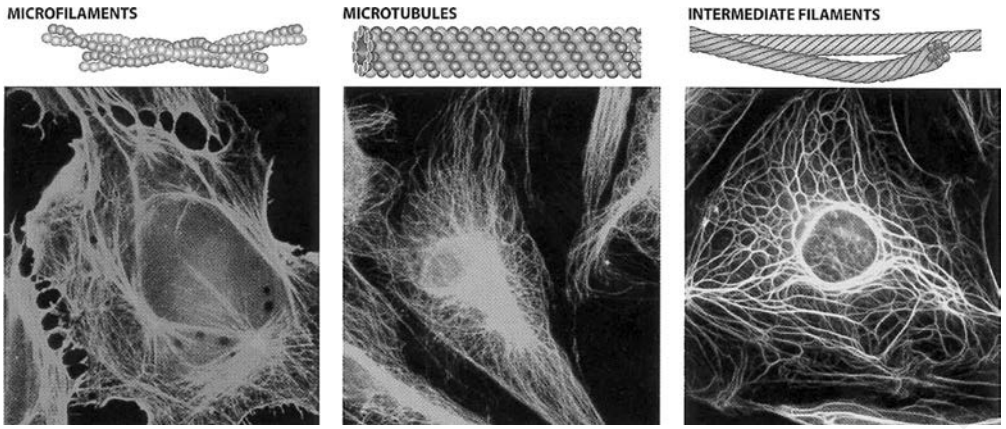

Fig. 1. Cytoskeleton polymer nets of living cell

with few groups of elements (one group being associated with one force density coefficient) but is seemingly difficult to extrapolate to structures comprising a large number of groups, particularly if the system is irregular.

On the other hand, the dynamic relaxation method appears to be more attractive in investigating nonregular tensegrity shapes. Indeed, it offers several possibilities for controlling the evolution of the form since we can specify a constant internal force in some elements and also act on the stiffness of each component, or both of these.

The aim of this paper is thus to illustrate the possibility of generating complex and various nonregular tensegrity systems by using this numerical method.

Interactive Form-Finding by Dynamic Relaxation Method

The form-finding process starts from an initial specified geometry. At the same time, self-stresses in some or all the components are arbitrarily specified. Hence, apart from particular cases or chance situations, the system cannot be in equilibrium. Hence the structure is set into motion by the unbalanced internal forces. The displacements are computed using the dynamic relaxation method based on calculating a sequence of decreasing energy peaks and this leads the system to reaching the steady equilibrium state. Even though this method is now well known, its basic principles will be summarized here to present the parameters chosen to generate irregular tensegrity shapes.

The equation governing the above motion is Newton's second law. For any node i in direction x at time t we have $R^t_{ix}=M_{ix}\ddot{V}^t_{ix}$, where R^t_{ix} is the residual internal force, M_{ix} a fictitious lumped mass associated to the components, and $\ddot{V}^t_{ix}$ nodal acceleration. Considering a central difference writing, the expression for acceleration at time t is

$$\ddot{V}^t_{ix} = 1/\Delta t(V^{t+\Delta t/2}_{ix} - V^{t-\Delta t/2}_{ix}) \tag{1}$$

where Δt=small time interval. The velocity at time $t+\Delta t/2$ can be rewritten as $V^{t+\Delta t/2}_{ix}=V^{t-\Delta t/2}_{ix}+\Delta t/M_{ix}R^t_{ix}$. The efficient value of $M_{ix}=\lambda/2\Delta t^2 S_{i\,\max}$ is given by the stability condition (Barnes 1988) where λ=convergence parameter constant for the whole structure; and $S_{i\,\max}$="nodal stiffness" associated with the stiffness of the components and is generally chosen as

$$S_{i\,\max} = \sum^{Ni} (EA/L_0 + T/L) \tag{2}$$

where N_i=number of elements connected to node i; EA/L_0=their axial linear stiffness (L_0 corresponds with the unstrained fabrication length), and T/L=their geometric stiffness (T and L=, respectively, force and length at the considered time).

The velocity is then $V^{t+\Delta t/2}_{ix}=V^{t-\Delta t/2}_{ix}+2R^t_{ix}/(\lambda\Delta t S_{i\,\max})$ and the new geometry at time $t+\Delta t$ is $x^{t+\Delta t}_t=x^t_i+\Delta t/V^{t+\Delta t/2}_{ix}$. Following this updating of geometry, the new force in an element is given by

$$T^{t+\Delta t} = T^s + (EA/L_0)^s(L^{t+\Delta t} - L^s) \tag{3}$$

where $T^s$and $(EA/L_0)^s$=, respectively, initial specified force and linear stiffness of the element; L^s and $L^{t+\Delta t}$=length at initial starting geometry and length at time $t+\Delta t$. The new residual force at node i is then

$$R^{t+\Delta t}_{ix} = \sum^{Ni} (T/L)^{t+\Delta t}(x_j - x_i)^{t+\Delta t} \tag{4}$$

The kinetic energy at the time increment $t+\Delta t/2$ can be expressed by $\Sigma^{\text{nodes}}1/2M_i(V^{t+\Delta t/2}_i)^2$. If the current kinetic energy is found to be less than the previous value, a peak has been passed. The velocities are then set to zero and node coordinates calculated at the time of this peak. This could be quadratically interpolated by considering the kinetic energy values at $t+\Delta t/2$, $t-\Delta t/2$, and $t-3\Delta t/2$ (Barnes 1988); the velocities at the midpoint of the first time step are given by $V^{\Delta t/2}=\Delta t/(2M)R^r$, R^r being the residual internal force at the restarting position.

The process repeats until the system reaches a steady equilibrium state according to a specified maximum outbalanced force. If in this resulting geometry some elements touch each other, which means that the system is not physically feasible, the

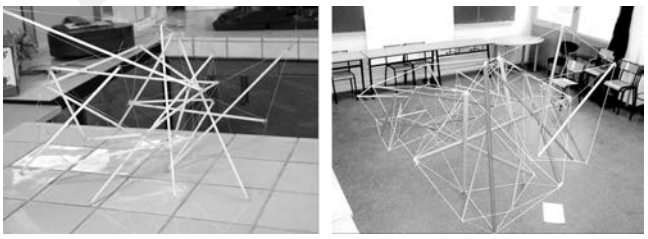

Fig. 2. Free-form tensegrity experimental physical models

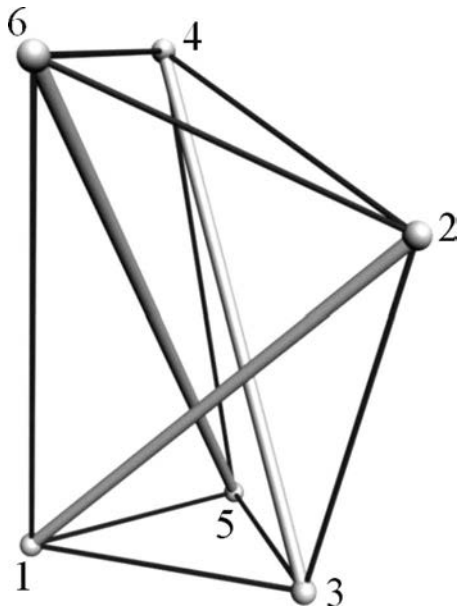

Fig. 3. Nonregular triplex

topology (removal of an element for instance) or the form (modification of some stiffness values) has to be modified until no contact occurs.

Strategies for Stiffness Choice

Three cases can be considered for choosing the value of EA for one element. This provides different ways of controlling the evolution of the resulting shapes. We will illustrate these features in the examples presented below.

1. Set EA to zero. The force in the element thus holds constant at the specified value T^s. In this case, we observe that the length of the element at final equilibrium state may vary radically when compared with its initial value. It must be emphasized that if the number of elements with a specified constant force increases, the chance of finding a corresponding equilibrated solution decreases.
2. Set EA to a realistic value. Since it is necessary here to specify the element unstrained length L_0, this value will offer the possibility of controlling the shape. Note that in this case, the modifications in lengths are smaller than in (1).
3. Set EA to a lower value compared to the other components (for example $EA=1000$ for struts and $EA=10$ for the element considered). This decreasing stiffness amplifies the influence of the L_0 value compared to situation (2) and, as a consequence, leads to greater effects on the final form. In general, modifying the L_0 of the elements with low stiffness was seen to provide effective control of the resulting shape of the system.

Applications

Nonregular Triplex

The system shown in Fig. 3 is an irregular triplex. Various situations will be compared in this example by considering different constant internal forces in some elements. Four cases are presented in Table 1; the associated constant self-stress values are written in bold numbers. The starting geometry is the same in all cases. We choose to set $EA=1000$ for struts and $EA=10$ for cables ($EA=0$ for the elements with an imposed force). In all our applications, we use $\Delta t=1, \lambda=1$ and a maximum outbalanced force of the system equal to 10^{-4} (all values are nondimensional). The calculation results are given in Table 1. They show that for the elements holding constant self-stress values, the final lengths vary radically compared with the initial lengths. This corresponds in fact to the necessary adjustment to reach the final equilibrium state.

Stella Octangula

The topology used for this application corresponds to one of D. Emmerich's proposals and is represented in Fig. 4 (Motro and Raducanu 2003; and Motro et al. 2002). The system is designed on the basis of a triangular antiprism: struts lie on the triangular bracing faces along the bisecting direction: one of their ends is an apex of a layer triangular face and the other end is in the second

Table 1. Element Forces and Lengths in Initial and Final States for Nonregular Triplex

	Self-stresses					Lengths				
		Final value					Final value			
Elements	Initial value	Case 1	Case 2	Case 3	Case 4	Initial value	Case 1	Case 2	Case 3	Case 4
1-2	−3.0	**−3.0**	−1.666	−1.390	−0.645	1.498	1.870	1.500	1.500	1.502
3-4	−3.0	**−3.0**	−2.045	−1.997	−0.806	1.977	1.962	1.979	1.979	1.982
5-6	−3.0	**−3.0**	−1.727	−1.647	−0.793	1.977	2.331	1.980	1.980	1.982
1-6	0.6	2.197	1.390	1.072	**0.600**	1.660	1.910	1.783	1.734	1.402
2-3	0.6	2.925	1.825	1.726	**0.600**	1.044	1.273	1.164	1.155	1.311
4-5	0.6	2.300	1.473	1.517	**0.600**	1.660	1.926	1.796	1.803	1.683
2-4	0.6	1.024	0.707	**0.600**	0.252	1.183	1.231	1.195	1.080	1.144
2-6	0.6	0.848	0.413	**0.600**	0.217	1.183	1.211	1.162	0.993	1.141
4-6	0.6	0.800	0.195	**0.600**	0.227	1.000	1.019	0.962	0.504	0.965
1-3	0.6	1.327	**0.600**	0.695	0.310	1.000	1.069	0.841	1.009	0.973
1-5	0.6	0.747	**0.600**	0.172	0.252	1.000	1.014	0.518	0.960	0.967
3-5	0.6	0.843	**0.600**	0.309	0.206	1.000	1.023	0.650	0.973	0.963

Note: Associated constant self-stress values are denoted by boldface.

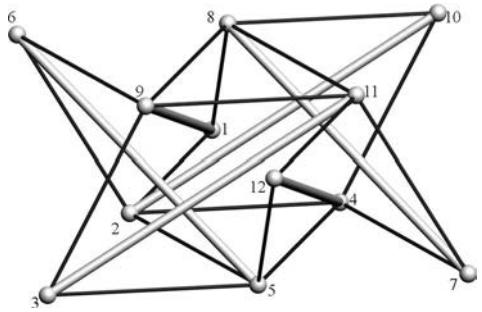

Fig. 4. Stella octangula

parallel plane. There are 6 struts, 18 cables connected to 12 nodes; for each strut one node is connected to two cables only and the corresponding equilibrium is thus realized into a plane. The length of struts is roughly 19 and roughly 11 for cables.

The equilibrium geometry is investigated by prescribing initial forces in strut and cable elements (−10 and 20, respectively). For struts the stiffness is $EA = 1000$ and for cables $EA = 10$. An equilibrium state is then obtained: the strut compressions are at present roughly −33 and the cable tensions roughly 19. Even if the process started with different specifications of initial forces, we observe that, in final equilibrium state, the absolute values of the ratio between the force and the reference length in all elements are almost the same (approximately 1.79).

The two examples above show that the dynamic relaxation method works effectively for finding an equilibrated state of tensegrity based on a given topology of a regular shape.

Free-Form Tensegrity

In this application, the final topology of the whole system is not fixed and specified in advance. The process starts from a simple structure and more and more elements are then added step by step. The computational sequence is the following: starting from a quadruplex (Fig. 5, a regular shape), another vertical strut 9–10 is next inserted (Fig. 6). To keep Nodes 9 and 10 in equilibrium state, it is necessary to add six cables (three connected to Node 9 and another three to Node 10). It is interesting to note that other possibilities exist for adding these new elements but we have chosen the simplest way. Following the same procedure, three other struts (11–12; 13–14; 15–16) and 18 cables are added to the system step by step; the topologies are shown in Fig. 7–9,

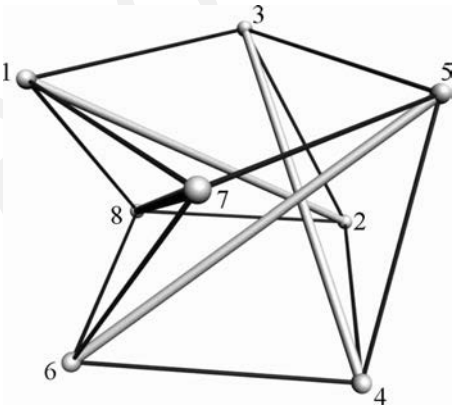

Fig. 5. Quadruplex tensegrity

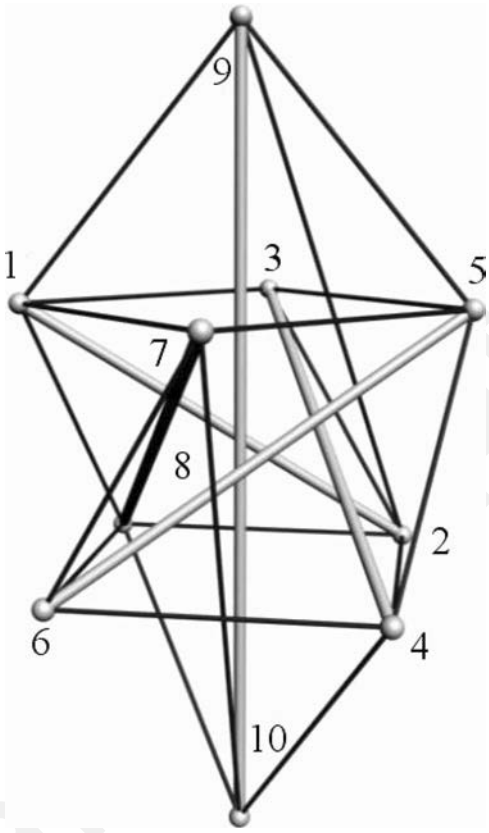

Fig. 6. Five-strut tensegrity module (new vertical strut is added in middle)

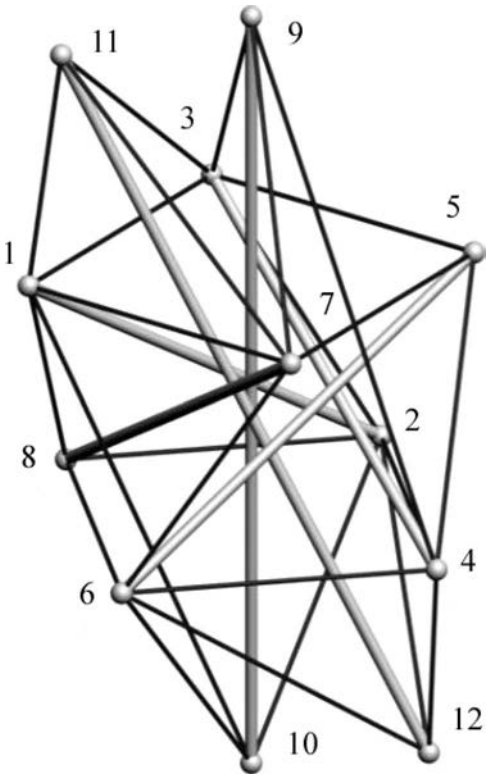

Fig. 7. Six-strut tensegrity module

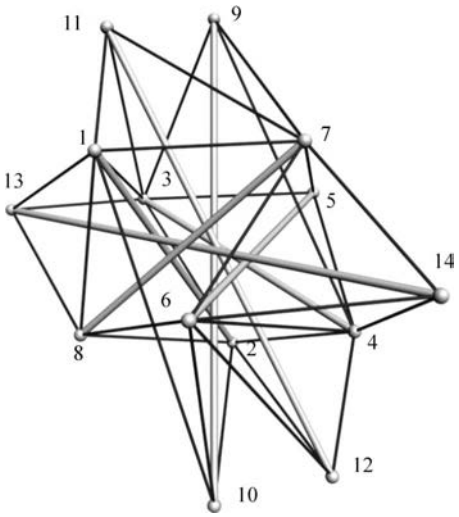

Fig. 8. Seven-strut tensegrity module

respectively. Finally, 8 struts and 36 cables are connected to 16 nodes.

Parameters $EA = 1000$ are now chosen for struts and $EA = 10$ for cables and an initial tension and compression specified for all cables and struts (2 and −1, respectively 1). An equilibrium state is then obtained with this given topology and data. In the resulting shape, a minimum distance of 0.481 is verified between any two spatial elements so that no contact occurs. Strut compression ranges from −2.854 to −4.328 and cable tension from 0.346 to 3.453. We observe that the tensions in Elements 2–4, 5–9, and 3–11 are, respectively, 0.640, 0.391, and 0.346, and are thus lower than the values in other cables. A topology analysis shows that there are more than three cables connected to Nodes 1, 2, 3, 6, 10, and 12. Since some of these elements can be regarded as redundant, they are removed from the system. This is the case for Cables 1–3, 6–10, and 2–12. Keeping all other parameters identical as previously, the form-finding process is then restarted. Finally, a new geometry is obtained (Fig. 10) with an equilibrated self-stress state. Strut compression ranges from −2.680 to −4.342 and cable tension from 0.758 to 3.049 with a minimum distance between elements equal to 0.611.

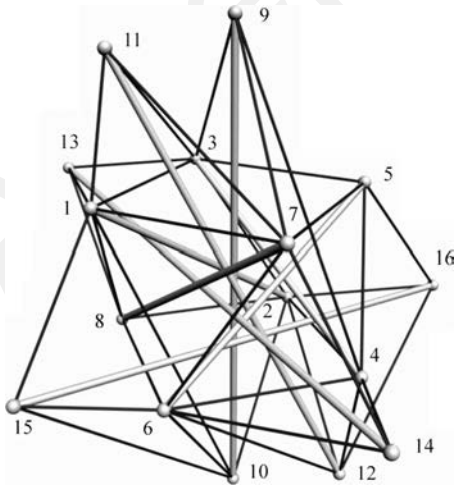

Fig. 9. Eight-strut tensegrity module

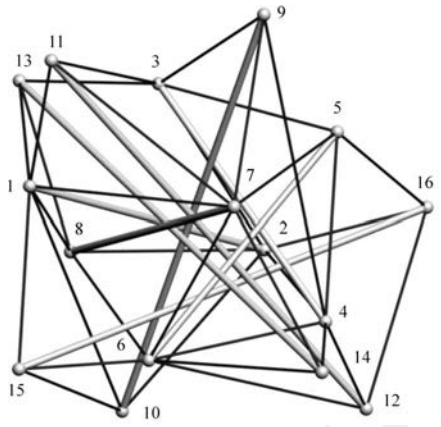

Fig. 10. Computed free-form tensegrity

In this example only two different lengths (19.998 and 32.950) are necessary for the eight struts at the starting configuration. During the form-finding process, one strut after another is added to the system randomly. To keep this strut stable, a number of cables are added to its ends. Many possibilities exist for such topology modifications and the designer can choose the most suitable solution.

Conclusion

There is a growing need for numerical methods devoted to form-finding in more complex, varied, and creative tensegrity shapes. The dynamic relaxation method can be used for this purpose since it provides control either of the force or of the length of an element by an appropriate choice of stiffnesses, giving the designer effective ways to guide the evolution of the system. Numerous applications are presented to illustrate the generation of nonregular tensegrity configurations and, thus, to show the efficiency of the process and the role of the chosen parameters. During the shape-finding process, the geometry or topology can also be altered. In the final equilibrium position, contact between elements may occur or some internal forces in an element change their sign (a cable could thus become a strut and vice versa). The system is hence not "topologically fixed" but may evolve so as to adapt itself to the successive equilibrium positions.

Notation

The following symbols are used in this paper:

A = cross-section area;
E = Young modulus;
L = actual current length;
L^s = length at initial starting position;
L_0 = unstrained fabrication length;
M_{ix} = fictitious lumped mass associated to node i;
N_i = number of elements connected to node i;
R^r = residual internal force at restarting position;
R^t_{ix} = residual (unbalanced) internal force;
$S_{i\,\max}$ = nodal stiffness;
T = actual internal force in element;
T^s = initial specified internal force in element;
V^t_{ix} = nodal velocity at time t;
$\dot{V}^t_{ix}$ = nodal acceleration;

x = displacement direction;
Δt = small time interval; and
λ = convergence parameter.

References

Barnes, M. R. (1988). "Form-finding and analysis of prestressed nets and membranes." *Comput. Struct.*, 30, 685–695.

Fest, E., Shea, K., and Smith, I. F. C. (2004). "Active tensegrity structure." *J. Struct. Eng.*, 130(10), 1454–1465.

Ingber, D. E. (1997). "Tensegrity: The architectural basis of cellular mechanotransduction." *Annu. Rev. Physiol.*, 59, 575–599.

Motro, R. (2003). *Tensegrity: Structural systems for the future*, Hermes, ed., Penton Science, U.K.

Motro, R., and Raducanu, V. (2003). "Tensegrity systems." *Int. J. Space Struct.*, 18(2), 77–84.

Motro, R., Smaili, A., and Foucher, O. (2002). "Form controlled for tensegrity form-finding Snelson and Emmerich examples." *Proc., Int. Symp. Lightweight Structures in Civil Engineering*, IASS, Poland, 243–248.

Nishimura, Y., and Murakami, H. (2001). "Initial shape-finding and modal analyses of cyclic frustum tensegrity modules." *Comput. Methods Appl. Mech. Eng.*, 190, 5795–5818.

Stamenović, D. (2005). "Effects of cytoskeletal prestress on cell rheological behavior." *Acta Biomaterialia*, 1(3), 255–262.

Sultan, C., Corless, M., and Skeleton, R. E. (2001). "The prestressability problem of tensegrity structures, some analytical solutions." *Int. J. Solids Struct.*, 38(30–31), 5223–5252.

Sultan, C., and Skelton, R. E. (2003). "Deployment of tensegrity structures." *Int. J. Solids Struct.*, 40(18), 4637–4657.

Vassart, N., and Motro, R. (1999). "Multiparametered form-finding method: Application to tensegrity systems." *Int. J. Space Struct.*, 14(2), 147–154.

Williamson, D., Skelton, R. E., and Han, J. (2003). "Equilibrium conditions of a tensegrity structure." *Int. J. Solids Struct.*, 40(23), 6347–6367.